

Experimental and Numerical Behaviour of CFST Columns with Longitudinal Stiffeners

Mohamed Ibrahim¹, Maher Elabd², Kamel Kandeel³

1 Teaching Assistant, Civil Engineering Department, Higher Institute of Engineering and Technology in Kafr El-sheikh, Mohamedrady202011@gmail.com

2 Lecturer, Civil Engineering Department, Faculty of Engineering, Menoufia University. m.elabd@sh-eng.menoufia.edu.eg

3 Professor of Steel Structures and Bridges, Civil Engineering Department, Faculty of Engineering, Menoufia University.

Abstract

The use of Concrete Filled Steel Tube CFST is increasingly implemented in the design of modern buildings for their high loading capacity and ductility compared to reinforced concrete or hollow steel columns if worked separately. Changes to structural usage may result in increasing the loads on building columns. This paper presents the experimental test results and non-linear finite element modelling of experimental test program carried on Concrete Filled Steel Tube CFST columns with longitudinal stiffeners as a proposed solution to increase the CFST capacity. The nonlinear analysis has been performed using ABAQUS and the finite element model is validated and verified against the test results conducted in this study. The study extends to include different parameters affecting the design of CFST columns by implementing the validated numerical model. The parameters include the stiffener shape, the number of stiffeners per specimen and the diameter to the tube thickness (D/t) ratio. Behaviour of experimental and numerical models is evaluated by monitoring the load-displacement and resulted deformation shapes. Results conclude that there is a slight increase in the load carrying capacity by adding longitudinal stiffeners that may encourage the use of such system for increasing the existing CFST columns.

Keywords: CFST, COMPOSITE, STEEL, COLUMNS.

NOMENCLATURE

D	External diameter of steel tube
D _{in}	Inner diameter of steel tube
L	Length of specimen
T	Thickness of steel tube
bs	Width of the steel stiffener
hs	Height of the channel steel stiffener
ts	Thickness of the steel stiffener
A _c	Cross-sectional area of concrete
A _{st}	Cross-sectional area of steel tube
A _{ss}	Cross-sectional area of steel stiffeners
A _s	Sum of cross-sectional areas of steel tube and stiffeners (=A _{st} + A _{ss})
f _y	Yield stress of steel tube
f _{cu}	Unconfined compressive cube strength of concrete
f _c	Unconfined compressive cylinder strength of concrete
f _{cc}	Confined compressive strength of concrete
E	Young's modulus
ε _c	Unconfined concrete strain
ε _{cc}	Confined concrete strain
P _{Test}	Ultimate load obtained from test
P _{FE}	Ultimate load obtained from finite element analysis

1. Introduction and literature review.

Concrete Filled Steel Tube columns (CFST) are widely used for high and low rise buildings due to their high strength and ductility. CFST columns are a typical composite structural system, due to the composite interaction between the steel tube and the included confined concrete, the advantages of the two materials can be utilized and their disadvantages can be avoided leading to a better performance for both components of the CFST column. In addition to the above advantages, the steel tubes surrounding the concrete columns help eliminating temporary formwork, which reduces construction time and workmanship costs. Furthermore, the steel tubes assist in carrying axial load as well as providing confinement to the concrete which make a great contribution in enhancing the strength of the filled concrete and the load capacity of these columns. However, the strength and behaviour of the composite columns are influenced by many parameters such as material strengths, tube shapes, diameter-to-thickness ratios of the tubes and depth-to-thickness ratios of the tubes. Local buckling is also one of the critical parameters affecting the strength of the concrete-filled tubular steel columns.

Several researches presented and discussed the behaviour and performance of CFST columns through experimental and numerical investigations. Experimental and analytical study on the behaviour of short CFST columns concentrically loaded in compression to failure was presented by Schneider [1]. The effect of the steel tube shape and wall thickness, tube tensile strength, tube diameter-to-thickness ratio, and concrete strength were experimentally and numerically investigated to determine their effect ultimate strength of the composite column [2-5]. Other Studies were presented to evaluate experimentally the load carrying capacity of CFST columns and the results compared with those obtained by Eurocode 4 (EC 4) and American Codes (AISC) [6-10] and found a good prediction of the axial strength of concrete filled steel tube columns. Recent experimental and numerical studies have been presented by many researchers [11-15] to achieve a numerical model capable of simulating the actual behaviour of CFST columns. The results from the finite element analysis and experimental results had been compared and showed a good agreement.

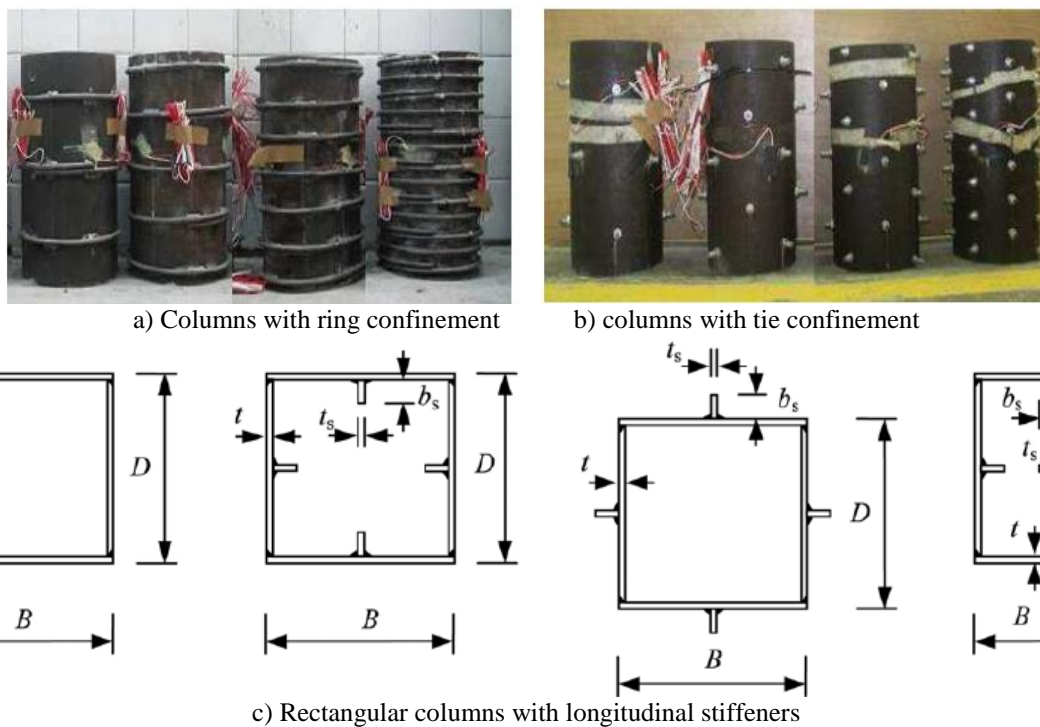


Fig.1. Ring and Tie confinement of CFST columns [16,17 and 18]

To determine the effect of adding external confinement in the form of rings and ties to the CFST to their loading capacity, a study was introduced by Johnny Ho [16] which concluded that there was no significant increase in the axial strength of the CFST column. However, using external confinement rings and ties improved enhanced the ductility before failure up to 20% besides increasing the stiffness of the column, see figure 1. Another study about confinement using the tie bars concluded that the ultimate load capacity and ductility of the columns was increased by using bar stiffeners [18]. Zhong Tao et al. [19, 20] studied the experimental behaviour of rectangular and square CFST columns with internal longitudinal stiffeners, see figure 1. They have concluded that the longitudinal stiffeners can not only delay the local buckling of the plate panel, but also improves the lateral confinement on the concrete core.

2. Experimental program and test setup

2.1 Experimental program description

A total of five specimens were prepared using circular mild steel tubes having a thickness of 2mm and 115mm diameter and cut to the required length of 250mm. All specimens were filled with fresh normal concrete of the same mix. Stiffeners are added to the section using continuous welding along the stiffener. The specimens were divided into three groups according the shape of stiffener. The first group had one specimen without stiffener as a reference specimen. The second group had two specimens with stiffeners of a plate shape. The stiffeners were of 10x2.0mm dimensions. The first specimen of the second group had six stiffeners while the other had eight stiffeners. The third group had two specimens with stiffeners which have channel shape, one of them had six stiffeners and the second had eight stiffeners. The stiffener channels were of thickness of 1 mm, web length 10 mm and flanges of 5 mm. The two shapes of the stiffeners had the same cross-section area of 20 mm². All stiffeners were equally spaced around the external perimeter of the steel tube. The cross section of specimens and the arrangement of stiffeners on perimeter column had shown on Figure 2. Photos of specimen were shown on Figure 3.

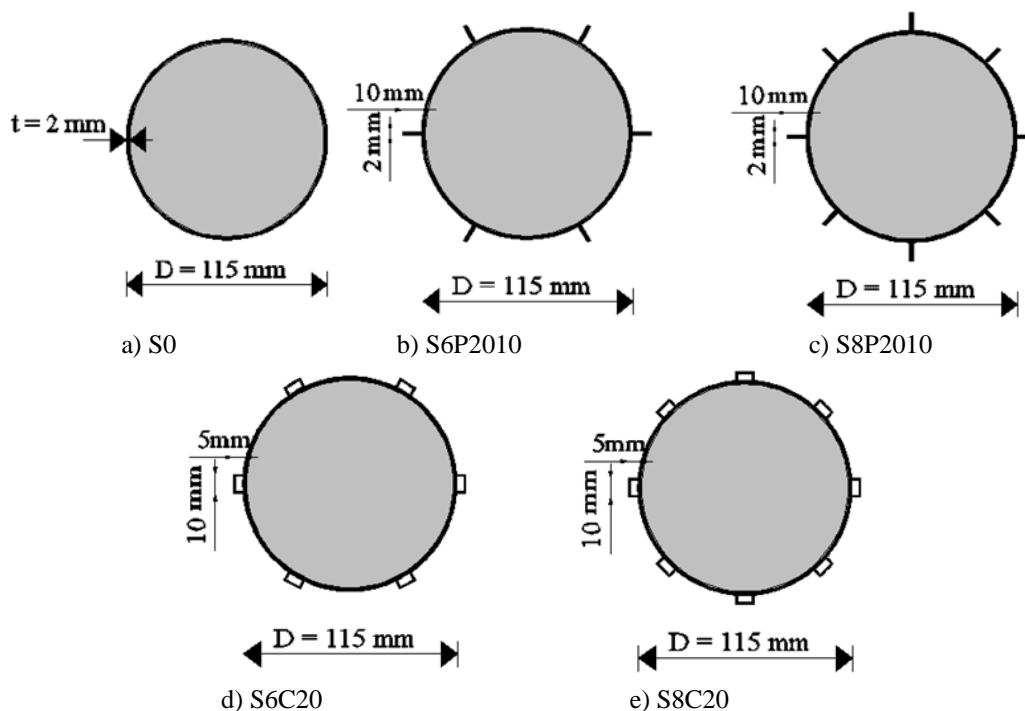


Fig. 2. The cross section of specimens and the arrangement of stiffeners on perimeter column

Table.1 summarizes the properties and details of specimens and stiffeners for each concrete-filled tubular steel column. The first specimen without any stiffeners labeled as S0. The specimens with longitudinal stiffeners labeled as S is for stub columns; the second letter labeled as 4, 6 or 8 for number of stiffener in specimen; the third letter labeled P or C is for the cross-section shape of stiffener (P stand for plate shape and C stand for channel); the Fourth and fifth letters labeled as 20 or 10 for cross-section area of stiffener in mm²; Sixth and seventh letters labeled as 10 or 5 for the length of plate stiffener.



Fig.3. Photos of specimens



Fig.4. Test setup of specimen

Table 1 Properties and details of specimens and arrangement of stiffeners

Specimen	Tube dimensions			No. of Stiff.	Area of stiffeners Ass (mm ²)	Area of tube Ast (mm ²)	Area of steel As (mm ²)	Stiffener Shape
	D (mm)	t (mm)	L (mm)					
S0	115	2	250	----	0	709.64	709.64	None
S6P2010	115	2	250	6	120	709.64	829.64	Plate
S8P2010	115	2	250	8	160	709.64	869.64	Plate
S6C20	115	2	250	6	120	709.64	829.64	Chanel
S8C20	115	2	250	8	160	709.64	869.64	Chanel

2.2 Preparation of physical models

The concrete used in filling the steel tubes had an average compressive strength (f_{cu}) of 30 MPa. The steel tubes and the stiffeners were made of mild steel with 360 MPa yield strength (f_y) and a Poisson's ratio of 0.3.

2.3 Test setup and instrumentation

The tests in this study were carried out in the laboratory of Menoufia University Faculty of Engineering using a compressive machine of 2000 KN Capacity. The specimens were prepared in the testing machine as shown in figure 4. A dial gauge was used to measure the axial displacement of the top head of the testing machine and was fixed parallel to the CFST axis.

2.4 Test procedures

The load was applied to the specimens in the form of axial uniform compression over the concrete and steel tube. The load was applied in a slow rate to avoid any high strain rates effects. The dial gauge and load readings were checked carefully recorded while loading was being applied to the specimens within the elastic limit. The load was applied at 10 KN intervals in order to have sufficient data points to delineate load-displacement curves. After the immediate drop of the load due to local duckling, the test continued as the load stabilized until the load started again to increase slightly when the testing ended. Then the specimen was removed and carefully examined after the test.

3. Experimental results

The axial load against axial displacement curves of concrete-filled tubular steel column specimens was drawn to discuss their behaviour. Comparisons between load capacities of specimens are presented. Ratios of increase in load capacity of columns due to using stiffener are compared with shape of stiffener and number of stiffener. The experimental load capacity of specimens and cross section area of specimens are shown in Table 2. The experimental load- displacement curves for all specimens are shown in figure 5 and 6

Table 2 the experimental load capacity of specimens.

Specimen	Concrete fcu (MPa)	Steel fy (MPa)	Area of steel As (mm ²)	PTest (kN)	Ratio of increase %
S0	30	360	709.64	580	-----
S6P2010	30	360	829.64	640	10.3
S8P2010	30	360	869.64	670	15.5
S6C20	30	360	829.64	630	8.6
S8C20	30	360	869.64	650	12

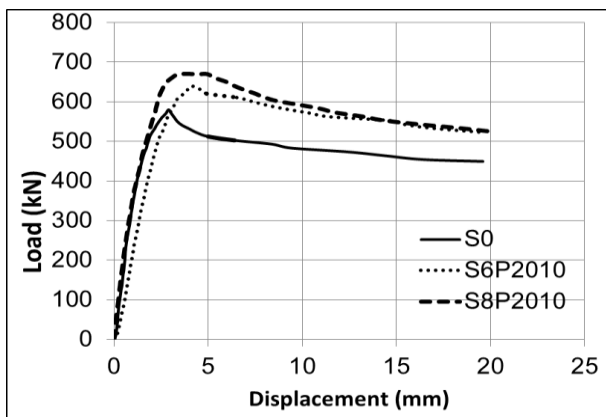


Fig.5. Experimental load-displacement curves for S0, S6P2010 and S8P2010.

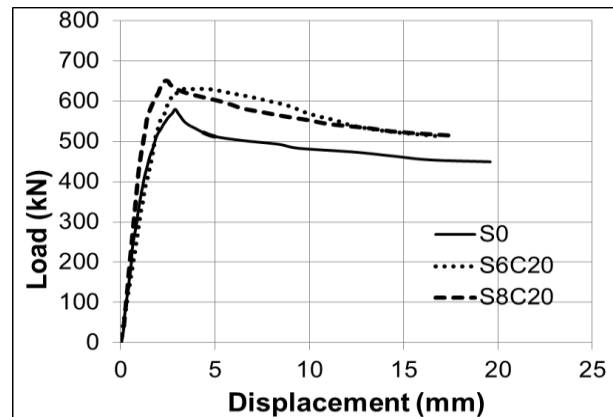


Fig.6. Experimental load-displacement curves for S0, S6C20 and S8C20.

Figure 7 show the failure mode of specimens and deformed shape at failure. It can be seen that both ends of the steel tube have locally buckled at failure under the loading plates. Also, by examining the specimen, the concrete was crushed. Therefore, the failure mode was confined concrete crushing and local buckling failure mode.

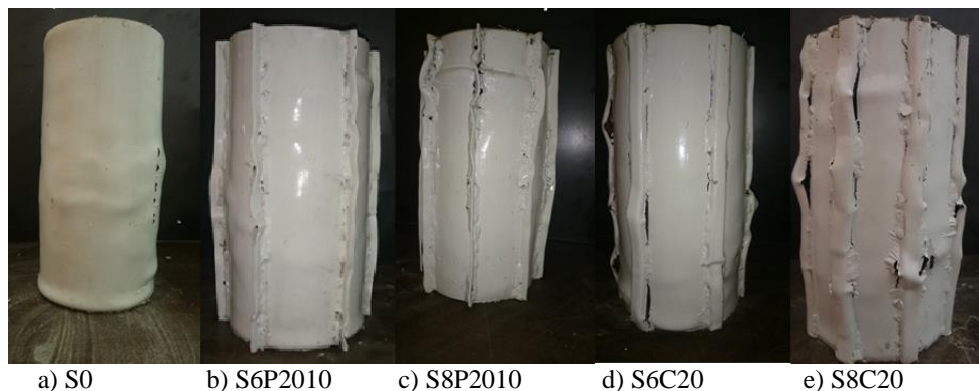


Fig.7. Experimental failure modes and deformed shapes at failure

4. Numerical Analysis

4.1 Validation of numerical model

4.1.1 General considerations

The main objective of this study is to develop an accurate finite element model to simulate the behaviour of CFST circular columns with longitudinal stiffeners. The finite element program ABAQUS [21] was used in current study. FE model depends on defining of the confined concrete, the steel tube and the interface between the normal concrete and the steel tube. In addition to these parameters, the choice of the element type, mesh size, boundary condition and load application.

4.1.2 Finite Element Type and Mesh

The steel tube and stiffeners were simulated by using the 4-noded doubly curved shell elements with reduced integration S4R. Fine mesh of three-dimensional 8-Node solid elements (C3D8) is used to model the concrete infilled and two end plates

4.1.3 Boundary Conditions and Load Application

All degrees of freedom for the top and bottom surfaces of CFST columns were prevented except for the displacement at the loaded end, which is the top surface, in the direction of the applied load. The STATIC option in ABAQUS was used to apply the load. The load was applied in increments using the modified RIKS method available in the ABAQUS library. The load will be defined as uniform load using PRESSURE option which is used to apply uniform load in the top surface of the upper plate.

4.1.4 Material Modeling of the Normal Confined Concrete

Modeling of concrete core required to define confined concrete as presented by Ellobody and Young [11]. Figure 8 shows the relationship between the equivalent uniaxial stress–strain curves for both unconfined and confined concrete. The defining of density and the stress-strain curve properties were required to modeling confined concrete. The stress-strain curve can also be distinguished in two parts (elastic part and plastic part). The linear part in the stress-strain curve of the normal concrete was defined by The ELASTIC option in ABAQUS. The elastic part properties are completely defined by giving the Young's modulus and the Poisson's ratio which was taken equal to 0.2. The plastic part of concrete was modeled using the DRUCKER PRAGER model available in ABAQUS [21]. The two parameters (*DRUCKER PRAGER and *DRUCKER PRAGER HARDENING) are used to define the yield stage of confined concrete. The linear Drucker Prager model is used with associated flow and isotropic rule. The material angle of friction (b) and the ratio of flow stress in triaxial tension to that in compression (K) are taken as 20° and 0.8, respectively, as recommended by Hu et al. [26].

4.1.5 Modeling of steel tube and longitudinal stiffeners

The modeling of the steel material requires defining the density, which was taken as 0.000078 kN/mm³, the linear part in the stress-strain curve of steel and nonlinear part of the curve. The elastic properties are completely defined by giving the Young's modulus, E, and the Poisson's ratio, the values of 210000 MPa and 0.3; respectively. The nonlinear part of the stress-strain curve of steel material was modeled using the PLASTIC option available in ABAQUS [21].

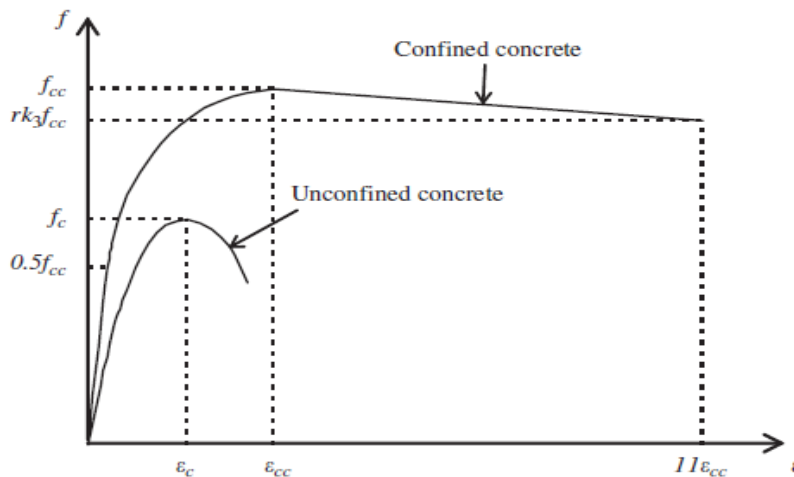


Fig.8. Equivalent uniaxial stress–strain curves for confined and unconfined concrete [11]

4.1.6 Modeling of concrete–steel tube interface

The interaction between the internal surface of the steel tube and the external surface of the concrete core is modeled by contact elements. The coefficient of friction between the two faces was taken as 0.25 in the analysis. The interface element allows the surfaces to separate under the influence of tensile force. However, both elements in contact are not allowed to penetrate each other by hard contact interface.

4.2 Proposed FE models

Twenty five specimens were modeling for study the behaviour of CFST with longitudinal stiffeners. Table 5 presented the summary of specimens. Specimens had the experimental properties like concrete strength $f_{cu}=30$ MPa and yield strength of steel $f_y=360$ MPa.

4.3 Validation process

The experimental and finite element results were compared to verify the finite element model. Comparisons were performed between the ultimate loads obtained from the tests (P_{Test}) and those obtained from the finite element analysis (PFE) as presented in Table 3. It can be seen that good agreement was achieved between the experimental and numerical results.

Table 3 Experimental and numerical ultimate loads comparison

Specimen	Tube dimensions			Shape of stiffener	PTest (kN)	PFE (kN)	$\frac{P_{Test}}{P_{FE}}$
	D(mm)	t(mm)	L(mm)				
S0	115	2	250	None	580	537	1.08
S6P2010	115	2	250	Plate	640	588	1.08
S8P2010	115	2	250	plate	670	603	1.1
S6C20	155	2	250	Channel	630	585	1.07
S8C20	155	2	250	Channel	650	593	1.09
Mean							1.08

The experimental and numerical load-displacement relationships for specimens S0, S6P2010, S8P2010, S6C20 and S8C20 were obtained as shown in Figures 9 to 13 respectively .It can be seen from both figures that generally good agreement was achieved. Comparisons between the deformed shapes from the tests and the finite element analysis for specimens S0, S6P2010, S8P2010, S6C20 and S8C20 were shown in figures 14. It was found that good agreement exists between the experimental and numerical deformed shapes of the columns .The failure mode observed experimentally confirmed the numerical prediction, which was mainly local buckling of the steel tube as well as crushing of the normal concrete.

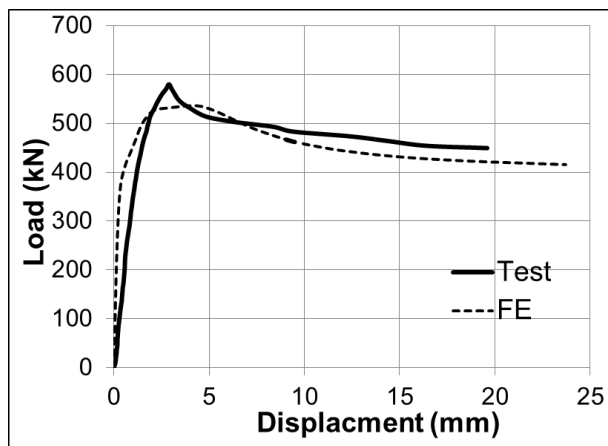


Fig.9. Experimental and numerical load-displacement for specimen S0

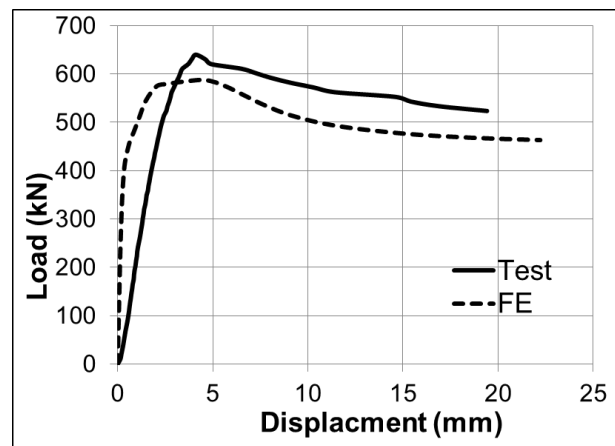


Fig.10. Experimental and numerical load-displacement for specimen S6P2010

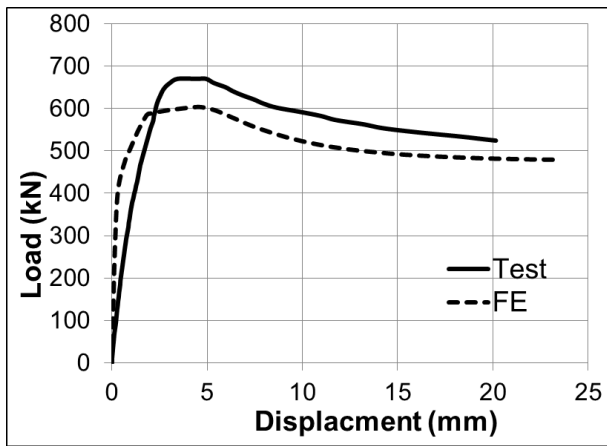


Fig.11. Experimental and numerical load-displacement for specimen S8P2010

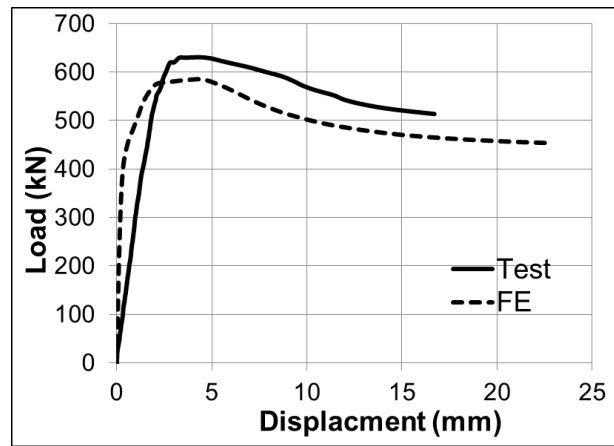


Fig.12. Experimental and numerical load- displacement for specimen S6C20

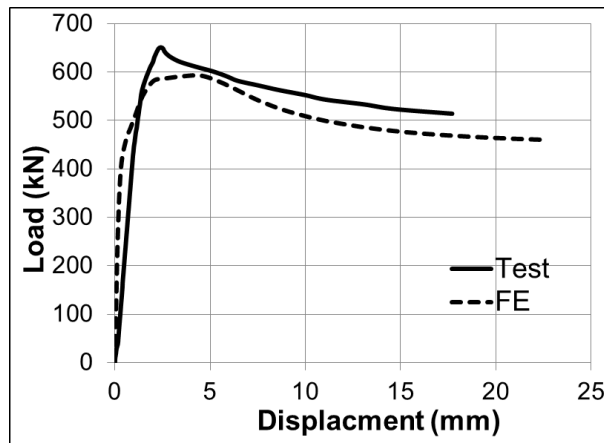


Fig.13. Experimental and numerical load-displacement for specimen S8C20

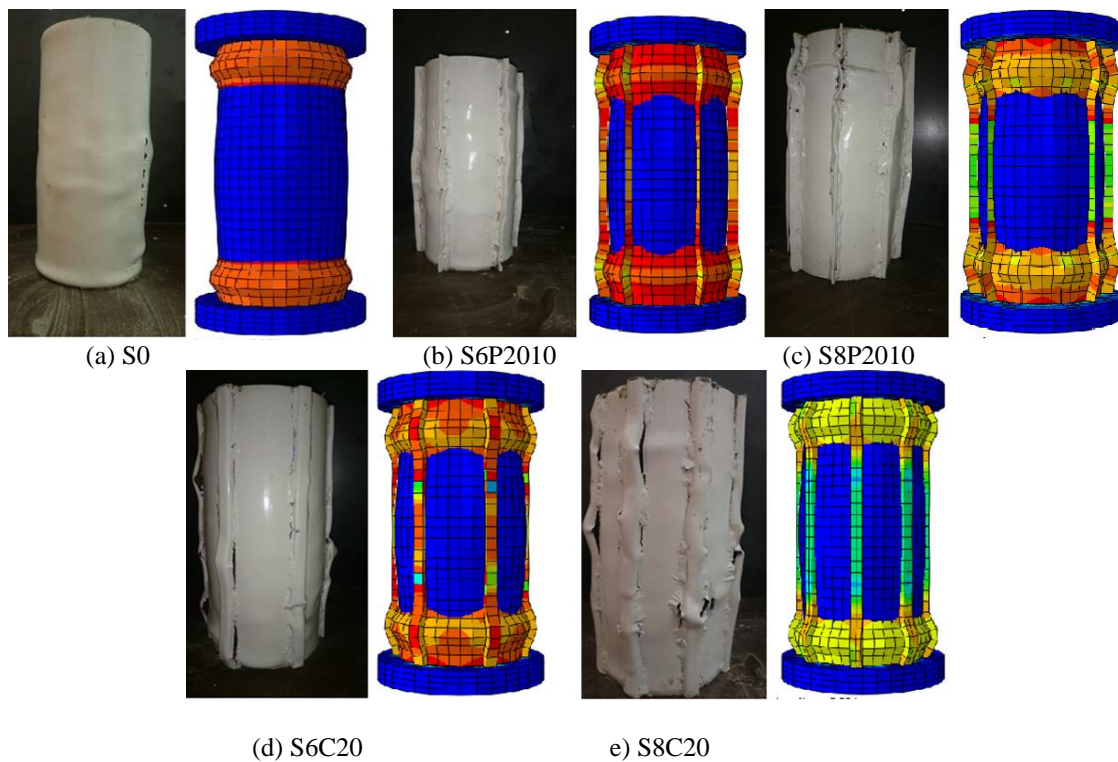


Fig.14. Experimental and numerical failure mode of the columns

4.4 Parameters of numerical study

Parametric study was performed using finite element to investigate the effects of different parameters affecting the behaviour of CFST circular columns with longitudinal stiffeners. The parameters include the cross-section area of steel and shape of stiffeners and their number. Stiffeners were regularly distributed on the perimeter of the column and the number of stiffeners was 4 or 6 or 8 per specimen. Six shape of stiffener were prepared with different cross area dimensions as presented in table 4. The study consists of 18 CFST columns with longitudinal stiffeners and 7 CFST columns without any stiffeners. Specimens were divided into six groups according to the cross-section area of steel. The cross-section area of steel was the sum of area of steel tube and area of stiffeners. Each group had 4 specimens the first specimen without stiffeners with bigger thickness; the other three specimens had the same area of stiffeners (20 or 10 mm²) number of stiffeners (4 or 6 or 8 per specimen). Tables 4&5 presents the specimen dimensions, number of stiffeners and cross-section area of steel, tube and stiffeners for each specimen. All specimens were filled with concrete of strength $f_{cu}=30$ MPa and yield strength for all steel elements was $f_y=360$ MPa.

Table 4 Cross-section shape and dimensions of plate stiffeners

Stiffener Label	Stiffener Shape	Cross-section area (mm ²)	Dimension	
			bs (mm)	ts (mm)
P2010	Plate	20	10	2
P205	Plate	20	5	4
P1010	Plate	10	10	1
P105	Plate	10	5	2

Table 4 Cross-section shape and dimensions of channel shape stiffeners

Stiffener Label	Stiffener Shape	Cross-section area (mm ²)	Dimension		
			hs (mm)	bs (mm)	ts (mm)
C20	Channel	20	10	5	1
C10	Channel	10	10	5	0.5

5. Analysis of Results and Discussion

The load capacity of columns which investigated in the first study is shown in table 5. The table presents the load capacity of columns which have the same cross-section area of steel as a group. The increasing ratios are presented in the Table 5 to compare between all shapes of stiffeners. Load –displacement curves are plotted for all specimens investigated in the study as shown in the figures 15 to 21. Load capacities of the CFST columns are increased due to the increase in numbers of stiffeners. The behaviour of the linear stage remained approximately constant for all specimens.

Comparisons between the load capacity of column and number of stiffeners are drawn for each stiffener shape as presented in Figures 22 and 23. The stiffener shapes consist of two groups. The first group has three shapes P2010, P205 and C20. The three shapes have the same cross-section area of one stiffener (20 mm²). The second group has stiffener P1010, P105 and C10. The three shapes have the same cross-section area of one stiffener (10 mm²).

Table 5 Specimen dimensions, number of stiffeners per specimen and load capacities of specimens

specimen	Specimen dimension			No. of Stiff.	Ass mm ²	Ast mm ²	As mm ²	Ac mm ²	PFE (kN)	Ratio of increase %
	Din (mm)	t (mm)	L (mm)							
D111t2.22	111	2.22	250	---	---	789.64	789.64	9672	564	
S4P2010	111	2	250	4	80	709.64	789.64	9672	573	1.59 %
S4P205	111	2	250	4	80	709.64	789.64	9672	576	2.13 %
S4C20	111	2	250	4	80	709.64	789.64	9672	565	0.18 %
D111t2.32	111	2.32	250	---	---	826.64	826.64	9672	578	
S6P2010	111	2	250	6	120	709.64	826.64	9672	588	1.73 %
S6P205	111	2	250	6	120	709.64	826.64	9672	593	2.6 %
S6C20	111	2	250	6	120	709.64	826.64	9672	585	1.21 %
D111t2.44	111	2.44	250	---	---	869.64	869.64	9672	589	
S8P2010	111	2	250	8	160	709.64	869.64	9672	603	2.37 %
S8P205	111	2	250	8	160	709.64	869.64	9672	607	3.05 %
S8C20	111	2	250	8	160	709.64	869.64	9672	593	.68 %
D111t2.11	111	2.11	250	---	---	749.64	749.64	9672	551	
S4P1010	111	2	250	4	40	709.64	749.64	9672	554	0.55 %
S4P105	111	2	250	4	40	709.64	749.64	9672	555	0.73 %
S4C10	111	2	250	4	40	709.64	749.64	9672	550	-0.18 %
D111t2.17	111	2.17	250	---	---	769.64	769.64	9672	558	
S6P1010	111	2	250	6	60	709.64	769.64	9672	562	0.72 %
S6P105	111	2	250	6	60	709.64	769.64	9672	563	0.9 %
S6C10	111	2	250	6	60	709.64	769.64	9672	556	-0.36 %
D111t2.22	111	2.22	250	---	---	789.64	789.64	9672	564	
S8P1010	111	2	250	8	80	709.64	789.64	9672	571	1.24 %
S8P105	111	2	250	8	80	709.64	789.64	9672	573	1.6 %
S8C10	111	2	250	8	80	709.64	789.64	9672	561	-0.53 %

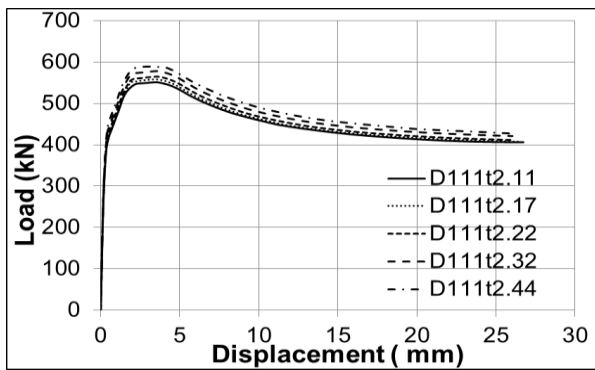


Fig. 15. Load-displacement curve for D111t2.11, D111t2.17, D111t2.22, D111t2.32 and D111t2.44

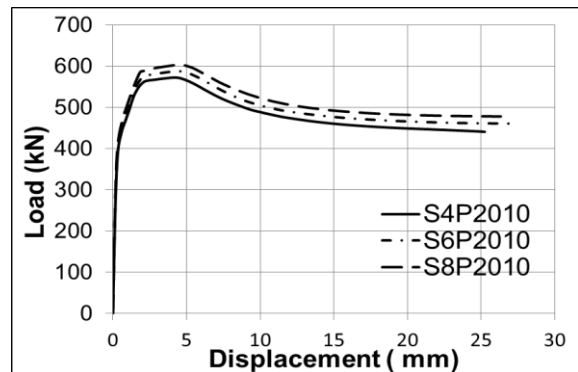


Fig. 16. Load-displacement curve for S4P2010, S6P2010 and S8P2010

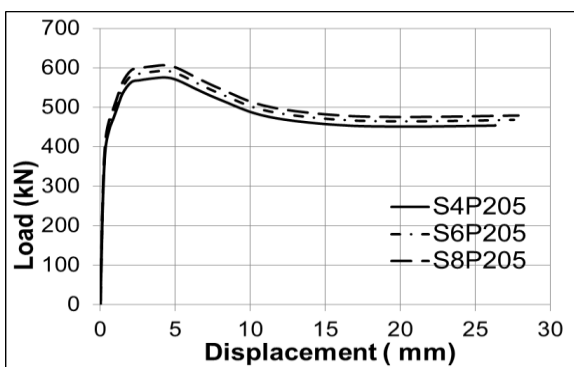


Fig. 17. Load-displacement curve for S4P205, S6P205 and S8P205

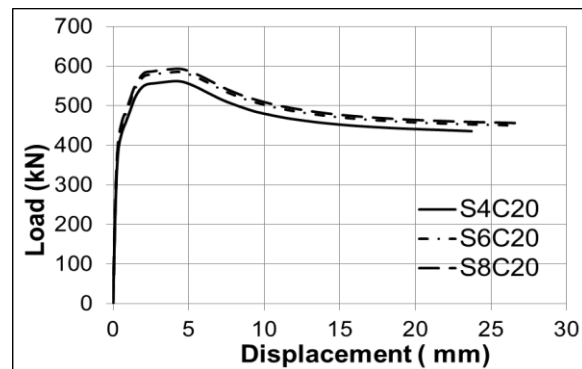


Fig. 18. Load-displacement curve for S4C20, S6C20 and S8C20

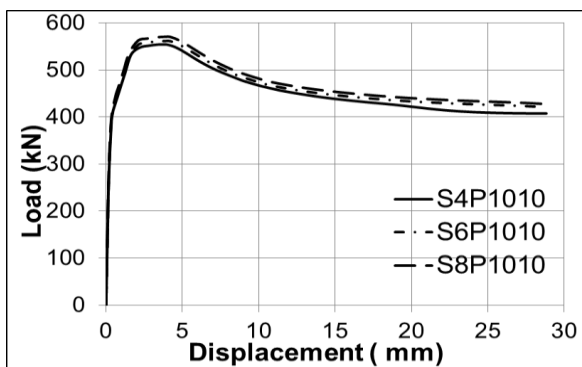


Fig. 19. Load-displacement curve for S4P1010, S6P1010 and S8P1010

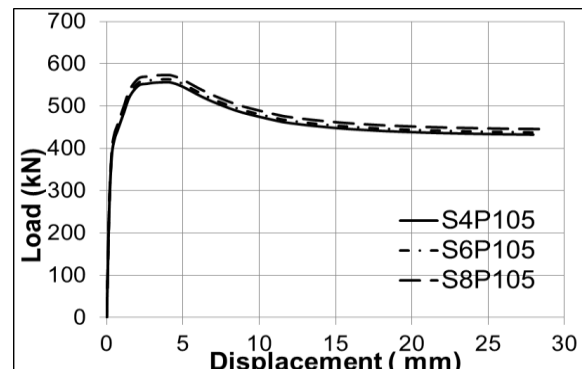


Fig. 20. Load-displacement curve for S4P105, S6P105 and S8P105

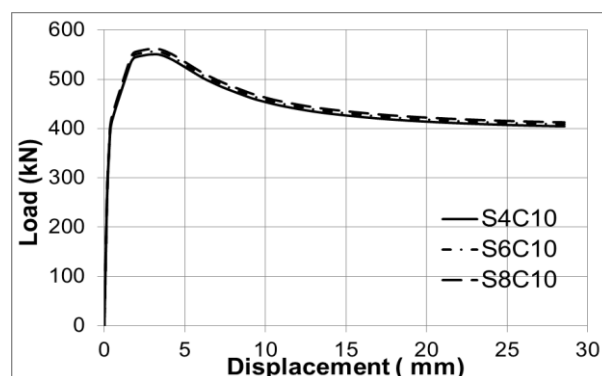


Fig. 21. Load-displacement curve for S4C10, S6C10 and S8C10

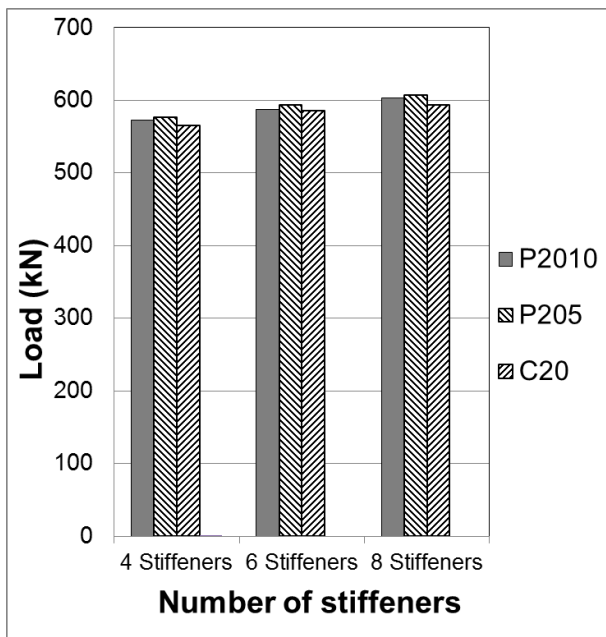


Fig.22. Load capacities of specimen and number of stiffeners (stiffener with area 20 mm²).

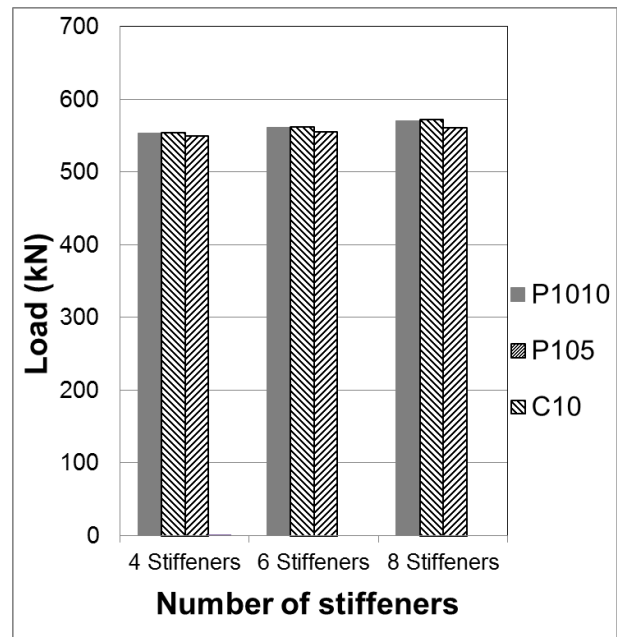


Fig.23. Load capacities of specimen and number of stiffeners (stiffener with area 10 mm²).

From figures 22 and 23, it can be noted that there is a slight increase in load capacity of column due to adding longitudinal stiffeners to CFST columns. This increase ranged between 0.18 % up to 3.05 %.

6. Conclusions

The current study presented the experimental test results of a group of tests conducted on CFST columns with added external longitudinal direction to monitor the changes in their behaviour and load capacity of such columns. The study also included an extensive parametric study using finite element for large number of parameters using ABAQUS. The parameters included the number of stiffeners, the type of stiffeners and the diameter to thickness ratio (d/t). The following conclusions can be summarized from the current study:

- 1) Adding longitudinal stiffeners to concrete-filled tubular steel column led to an increase in the load carrying capacity of CFST columns by a ratio that ranged from 0.18% to 3.05%.
- 2) The load carrying capacity of CFST columns increased by increasing the number of stiffeners.
- 3) The existence of longitudinal stiffeners led to more ductile behaviour of CFST compared to convention concrete-filled tubular steel columns (CFST without stiffeners).
- 4) In general, using plates as stiffeners was better than using stiffeners of channel cross section.
- 5) The largest increase was achieved by using stiffeners of plate cross section shape with shortest length and large thickness.

7. References

- [1] Schneider, S. P., “Axially Loaded Concrete-filled Steel Tubes”, *Journal of Structural Engineering*, ASCE, Vol. 124, No. 10, pp. 1125-1138, 1998.
- [2] O’Shea, M. D., and Bridge, R. Q., “Design of Circular Thin-Walled Concrete Filled Steel Tubes”, *Journal of Structural Engineering*, ASCE, Vol. 126, No. 11, pp. 1295-1303, (2000).
- [3] Sakino, K., Nakahara, H., Morino, S., and Nishiyama, I., “Behavior of Centrally Loaded Concrete-Filled Steel-Tube Short Columns”, *Journal of Structural Engineering*, ASCE, Vol. 130, No. 2, pp. 180-188, (2004).
- [4] Yu, Z., Ding, F. and Cai, C., “Experimental Behavior of Circular Concrete-filled Steel Tube Stub Columns”, *Journal of Constructional Steel Research*, Vol. 63, pp. 165–174, (2007).
- [5] Gupta, P. K., Sarda, S. M., and Kumar, M. S., “Experimental and Computational Study of Concrete Filled Steel Tubular Columns under Axial Loads”, *Journal of Constructional Steel Research*, Vol. 63, pp. 182-193, (2015).
- [6] Lam, D. and Gardner, L., “Structural Design of Stainless Steel Concrete Filled Columns”, *Journal of Constructional Steel Research*, Vol. 64, No.11, pp. 1275-1282, (2008).
- [7] Kuranovas, A., Goode, D., Kvedaras, A. and Zhong, S., “Load-Bearing Capacity of Concrete-Filled Steel Columns”, *Journal of Civil Engineering and Management*, Vol. 15, No.1, pp. 21-33, (2009).
- [8] Bedage, S. D, and Shinde, D. N., “Concrete Filled Steel Tubes Subjected to Axial Compression”, *International Journal of Research in Engineering and Technology*, Vol. 4, No. 6 pp. 459-464, (2015).
- [9] Giakoumelis, G, Lam, D., “Axial Capacity of Circular Concrete-filled Tube Columns”, *Journal of Constructional Steel Research*, Vol. 60, pp. 1049–1068, (2004).
- [10] Zhong, T., Wang, Z. and Yu, Q., “Finite Element Modeling of Concrete-filled Steel Stub Columns under Axial Compression”, *Journal of Constructional Steel Research*, Vol. 89, pp. 121–131,(2013) .
- [11] Ellobody, E., “Nonlinear Behavior of Concrete-filled Stainless Steel Stiffened Slender Tube Columns”, *Journal of Thin-Walled Structures*; Vol. 45, No. 3, pp.259–73, (2007).
- [12] Ellobody, E., “Nonlinear Behaviour of Concrete-filled Stainless Steel Stiffened Slender Tube Columns”, *Journal of Thin-Walled Structures*; 45(3):259–73(2007).
- [13] Ellobody, E., “Buckling Analysis of High Strength Stainless Steel Stiffened and Unstiffened Slender Hollow Section Columns”, *Journal of Constructional Steel Research*, Vol. 63, No. 2, pp. 145–55,(2007).
- [14] Han, H., Liu, W. and Yang, Y., “Behavior of Concrete-filled Steel Tubular Stub Columns Subjected to Axially Local Compression”, *Journal of Constructional Steel Research*, Vol. 64, No. 2 pp. 377–387(2008).
- [15] Abed, A., AlHamaydeh, M. and Abdalla, S., “Experimental and Numerical Investigations of The Compressive Behavior of Concrete Filled Steel Tubes (CFSTs)”, *Journal of Constructional Steel Research*, Vol. 80, pp. 429–439,(2013)
- [16] Ching, J. and Ho, M., “Improved behavior of concrete-filled-Steel-tube columns with external confinement”, *Journal of Procedia Engineering*, Vol. 4, pp. 662 – 669, (2011).
- [17] Laia, M. and Ho, J., “Axial Compression Test of Concrete-Filled-Steel-Tube Columns Confined by Tie Bars”, *Journal of Procedia Engineering*, Vol. 57, pp. 662 – 669, (2013).
- [18] Bahrami, A., Hamidon, W. and Osman, A., “Behavior of Stiffened Concrete-filled Steel Composite (CFSC) Stub Columns”, *Latin American Journal of Solids and Structures*, Vol. 10, pp. 409 – 440, (2013) .
- [19] Tao, Z., Han, L. and Wang, Z., “Experimental Behavior of Stiffened Concrete-filled Thin-Walled Hollow Steel Structural (HSS) Stub Columns”, *Journal of Constructional Steel Research*, Vol. 61, pp. 962–983, (2004).
- [20] Tao, Z., Uy, B., Han, L. and Wang, Z., “Analysis and Design of Concrete-filled Stiffened Thin-Walled Steel Tubular Columns under Axial Compression”, *Journal of Thin-Walled Structures*, Vol. 47, pp. 1544–1556, (2009).
- [21] ABAQUS Standard User’s Manual (2004), Vol. 1–3. Version 6.4. USA: Hibbitt, Karlsson and Sorensen Inc.
- [22] ACI. Building Code Requirements for Structural Concrete and Commentary (1995), ACI 318-95. Detroit (USA): American Concrete Institute.
- [23] Mander, J.B., Priestley, M., and Park R., “Theoretical Stress–Strain Model for Confined Concrete”, *Journal of Structural Engineering*, ASCE, Vol. 114, No. 8, pp. 1804–1826, (1988).
- [24] Richart, F., Brandzaeg, A. and Brown A., “Study of The Failure of Concrete under Combined Compressive Stresses”, Bull. 185. Champaign (Illinois, USA): University of Illinois Engineering Experimental Station. (1928).
- [25] Hu H.T., Huang C.H., Wu M.H., and Wu Y.M., “Nonlinear Analysis of Axially Loaded Concrete-filled Tube Columns with Confinement Effect”, *Journal of Structural Engineering*, ASCE, Vol. 129, No. 10, pp. 1322–1329, (2003).
- [26] Hu, H.T., Schnobrich W.C., “Constitutive Modeling of Concrete by Using Nonassociated Plasticity”, *Journal of Materials in Civil Engineering* , Vol. 1, No. 4, pp. 199–216, (1989).
- [27] Saenz L.P., Desayi, P. and Krishnan, S., “Discussion of Equation for the Stress–Strain Curve of Concrete”, *Journal of the American Concrete Institute*, Vol. 61, pp. 1229–1235, (1964).
- [28] Giakoumelis, G, Lam, D., “Axial Capacity of Circular Concrete-filled Tube Columns”, *Journal of Constructional Steel Research*, Vol. 60, pp. 1049–1068, (2004).
- [29] Eurocode 4. Design of composite steel and concrete structures. Part 1.1, General rules and rules for buildings (with UK national application document), DD ENV 1994-1-1. London (UK): British Standards Institution,(1994).